Journal of Hazardous Materials 162 (2009) 906–912

Contents lists available at ScienceDirect

Journal of Hazardous Materials

journal homepage: www.elsevier.com/locate/jhazmat

Enhanced degradation of *p*-chlorophenol in a novel pulsed high voltage discharge reactor

Wenjuan Bian*, Xiangli Ying, Junwen Shi

School of Chemistry and Chemical Engineering, Soochow University, Suzhou 215123, China

ARTICLE INFO

Article history:
Received 29 July 2007
Received in revised form 25 May 2008
Accepted 26 May 2008
Available online 7 June 2008

Keywords:
Discharge in water
Active species
p-Chlorophenol
Degradation

ABSTRACT

The yields of active specie such as ozone, hydrogen peroxide and hydroxyl radical were all enhanced in a novel discharge reactor. In the reactor, the original formation rate of hydroxyl radical was 2.27×10^{-7} mol L^{-1} s^{-1}, which was about three times than that in the contrast reactor. Ozone was formed in gas-phase and was transferred into the liquid. The characteristic of mass transfer was better in the novel reactor than that in the contrast reactor, which caused much higher ozone concentration in liquid. The dissociation of hydrogen peroxide was more evident in the former, which promoted the formations of hydroxyl radical. The *p*-chlorophenol (4-CP) degradation was also enhanced. Most of the ozone transferred into the liquid and hydrogen peroxide generated by discharge could be utilized by the degradation process of 4-CP. About 97% 4-CP was removed in 36 min discharge in the novel reactor. Organic acids such as formic, acetic, oxalic, propanoic and maleic acid were generated and free chloride ions were released in the degradation process. With the formation of organic acid, the pH was decreased and the conductivity was increased.

1. Introduction

Pulsed high voltage discharge in water has been used for wastewater treatment for many years, demonstrating that it could induce an oxidation process for organic contaminants degradation in aqueous solution [1–3]. The basic mechanism of the oxidation process is the formations of plasmas, which can promote both physical and chemical processes leading to strong UV light, local high temperature and intense shock waves and the formations of chemically active species such as $^{\bullet}OH$, $H^{\bullet}$, $O^{\bullet}$, $O_2^{\bullet-}$, $HO_2^{\bullet}$, H_2O_2, O_3, respectively, etc. [4–12]. The pulsed high voltage discharge in water does not need any aids, and it is a combination of chemical, photochemical, ultrasonic and electrical process.

In the pulsed high voltage discharge system, the structure of the discharge reactor, which was decided by the configuration of the discharge electrode and ground electrode, could influence the formation of active species and organic degradation [13,14]. In an atomizer reactor used for removal dichlorophenol, the chamber consisted of a hollow, Teflon-coated Lucite cylinder with a set of axially oriented intermeshed electrodes placed in the center [15]. A 6.1 mmol aqueous dichlorophenol sample was cycled through the reactor six times, resulting in the release of 55% of the initial dichlorophenol chloride ions. Willberg and Lang designed a rod–rod reactor with two electrodes submerged into water to degrade the 2,4,6-trinitrotoluene [16,17]. 165 μmol solutions were completely mineralized over the course of 300 electrical discharges of 7 kJ each. A reactor with ring-to-cylinder electrode geometry was developed to treat dye solutions of Rhodamine B, Methyl orange, and Chicago sky blue by Sugiarto et al. [14]. The removal ration was about 90% and was increased in the presence of hydrogen peroxide with an initial pH of 3.5. Sano et al. used a cylindrical anode discharge reactor modified from a plate anode reactor to decompose aqueous phenol, resulting in an increase in electron efficiency and energetic efficiency of 2–3 and 3–4 times [13,18]. In a reactor with two parts, i.e., electrostatic atomization part and corona discharge reactor part, the Chicago sky blue was effectively decolorized by a combination of electrostatically atomized dye solution and the pulsed streamer corona discharge [19]. Li et al. carried out their research in a gas–liquid-phase pulsed discharge plasma reactor [20]. A rectangle stainless mesh was put in a ceramic tube as discharge electrode. The additive gas was transmitted to the inside of ceramic tube through silicone tube-coated on the back of ceramic tube to avoid edge effect and entered into solution through tiny holes on the ceramic tube. 50 ppm phenol with 200 mL original volume was removed almost completely after discharge for 120 min.

The needle-plate reactor was presented early [1]. The discharge electrode was consisted of one or several needles, which are hollow or solid. The gas was bubbled through the inner channel of

* Corresponding author. Tel.: +86 512 65880089; fax: +86 512 65880089.
E-mail addresses: bwenjuan@suda.edu.cn, bwenjuan@yahoo.co.cn (W. Bian).

0304-3894/$ – see front matter © 2008 Elsevier B.V. All rights reserved.
doi:10.1016/j.jhazmat.2008.05.156

the hollow needles or through the aeration tubes covering the solid needles. The configuration of the ground electrode was planar, whose diameter was much less than the inside diameter of the reactor body. The needle-plated reactor with the two electrodes all submerged into water was used by many researchers [1–3,21–24]. It was confirmed that some organics such as phenol, anthraquinone dye were effectively removed in the reactor. When bubbling oxygen into the reactor, the ozone was detected during discharge [1]. Sun et al. investigated the characteristics of the discharge and the active species, resulted that hydroxyl radical was formed mainly within the discharge channel, and the yields of •OH and H_2O_2 was higher in the case of spark discharge than that in the streamer corona discharge when the input energy was the same [2]. The degradation of phenol with the addition of gas bubbling and chemicals was investigated in a needle-plated reactor, which resulted in oxygen gas bubbling, and the addition of a small amount of hydrogen peroxide greatly increased the degradation rate of phenol [9]. Joshi et al. determined the formation rate of hydroxyl radical and hydrogen peroxide in a needle-plate reactor of 550 mL [4]. The hydroxyl radical formation rate was 1.019×10^{-9} mol L^{-1} s^{-1} and the hydrogen peroxide formation rate was 1.567×10^{-7} mol L^{-1} s^{-1} at average power input of 154 W L^{-1}. As high voltage needle-point electrodes were submerged in the aqueous-phase coupled with planar ground electrode suspended in the gas-phase above the water surface, hybrid gas–liquid electrical discharge was induced. Lukes et al. studied the character of the hybrid gas–liquid electrical discharge [25]. The formation rate of hydrogen peroxide was 4.9×10^{-7} mol s^{-1}. The hydroxyl radical and ozone were the key oxidation species produced by the gas-phase discharge of the hybrid-series reactor under argon and oxygen atmosphere and degradation of substituted phenol was found to follow first-order kinetics [26]. Grymonpré et al. analyzed the removal of low concentration of phenol in this reactor, found that 0.21 mg L^{-1} O_3 was produced at 60 min in a potassium chloride solution [27]. The amount of hydrogen peroxide formed in the liquid-phase was the same in the reactor with a gas gap containing oxygen as in the case when both electrodes were submerged in the liquid-phase, which was about 2.1 mmol L^{-1} at 60 min discharge. Zhang et al. carried out their research in a hybrid gas–liquid electrical discharge reactor with pumping compressed air into the air chamber though an air inlet tube to the discharge region [28]. Sahni and Locke determined the production of hydroxyl radical in three different reactor configurations: purely liquid-phase discharge, hybrid-series and hybrid-parallel [29]. The hybrid reactors with the additional discharge in the gas-phase result in greater production of hydroxyl radical when compared to the purely liquid-phase discharge. The influence of the initial solution conductivity on the production of hydroxyl radical is more pronounced for the purely liquid-phase discharge reactor in comparison to the hybrid configurations, with the hybrid-series showing the least influence. They also demonstrated that the concentration of chemical probe had strong effects on the measurements of hydroxyl radical generation [30]. The measured rate of production of hydroxyl radical increased but the production of hydrogen peroxide decreased with the increase in the concentration of the probe.

In the present study, a novel reactor is developed over the previous needle-plated reactor. The formation of hydroxyl radical, hydrogen peroxide and ozone is much increased. With the increase in the active species, the degradation of organic contaminant could be sped up. In addition to emphasizing on the yields of active species in two different reactors, the aim of the paper is to study the enhanced degradation process of 4-CP. Some organic acid will be generated and free chloride ions will be released in 4-CP degradation process, which could cause a variation in the pH and conductivity.

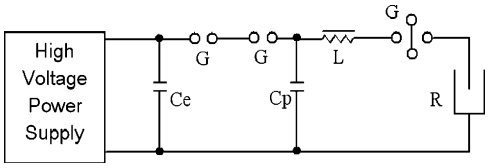

Fig. 1. The sketch of the pulsed high voltage source.

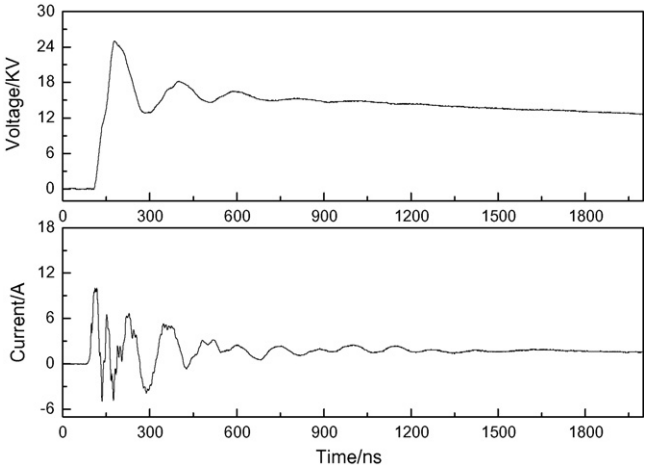

Fig. 2. The waveform of voltage and current input into the reactor by the pulsed power source.

2. Materials and methods

2.1. Materials

The power supply was realized by making use of rotating spark gap to produce pulsed high voltage (Fig. 1). It consisted of a DC high voltage producer (0–50 kV), a pulsed capacitance (C_p, 1.2 nF), a filter capacitor (C_e, 1 μF) and a rotational spark gap (G). The instantaneous voltage input into the reactor by the power supply is shown in Fig. 2. The rise time and width of the voltage was not more than 200 and 500 ns, respectively.

The diagram of the pulsed high voltage discharge system is shown in Fig. 3. The discharge reactor was made of organic glass with a diameter of 75 mm. The two sets of electrodes were placed in water. The lower system was connected with the output of the pulsed high voltage and consisted of five acupuncture needles (steel, Φ 0.25 mm) which were covered by capillaries through which gas was supplied to the discharge region, forming gas bubbles. The inner diameter of the five capillaries was 1.0 mm. The bubbling gas was bubbled into the little air chamber from a steel cylinder filled with pure oxygen. The gas flowed through the five capillaries and into the liquid chamber. The flow rate was kept at 120 L h^{-1} there was no specific note. In the case of non-bubbling,

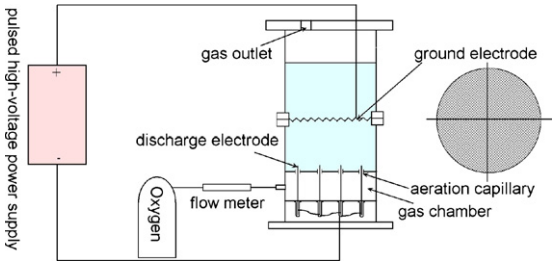

Fig. 3. The schematic of pulsed high voltage discharge system.

the aeration capillaries were encapsulated by 504 glues, which is a developed adhesive used synthetic resin as the main material and solidified agent as auxiliary material, otherwise the condition was the same. The needle tips were 0.5 mm higher than the upper end of the capillaries. The ground electrode was stainless steel wire mesh (30 mesh × 30 mesh; aperture, 0.61 mm) in reactor I. In the contrast reactor (reactor II), the ground electrode was a stainless steel plate with a diameter of 60 mm and the others were same. In all experiments, the applied voltage was 25 kV at 140 Hz. The electrode distance was 20 mm. After the gas flux was stabilized, 300 mL of certain solution was poured into reactor through upper end of the rector. When the voltage was adjusted to a suitable value, the experiment began. 1.0 mL of the sample was taken out of reactor at an interval of 3 or 6 min. All experiments were conducted three times and gave reproducibility within 6%.

2.2. Analysis methods

4-Hydroxybenzoate (HDB) was chosen as the probe for the advantage that 3,4-dihydroxybenzoic acid (DHDB) is the only isomer of quantitative reaction between HDB and •OH [31]. Therefore, an indirect method was used for determining •OH formation rate [31,32].

All reagents were used as received. 4-Hydroxybenzoate (HDB), 3,4-dihydroxybenzoic acid (DHDB) and 4-CP were analyzed by HPLC (Waters 515-996), equipped with a MS-2 C_{18} column (Φ 4.6 mm × 250 mm) and a photodiodc Array detector. The mobile phase was prepared by dissolving 1 mL L^{-1} H_3PO_4 and methanol. The ratio (v/v) was 50/50.

H_2O_2 was determined by a UV–vis Spectrophotometry (TU-1810) at wavelength of 400 nm [33]. O_3 was also measured by a Spectrophotometric method [34,35]. The organic acids and free chloride ions were determined by a Metrohm 861 Advanced Compact Ion Chromatograph equipped with an ASSUP 5 column (4.0 mm × 250 mm). The mobile phase was composed of sodium carbonate (1.0 mmol L^{-1}) and sodium bicarbonate (3.2 mmol L^{-1}) with a flow rate of 0.7 mL min^{-1}. The conductivity and pH was determined by a Conductivity meter (DDS-11 A) and a pH meter (PHS-3C).

The waveform of current and voltage input into the reactor were measured with a digital oscilloscope (TDS2014) produced by Tektronix, which had a high voltage probe (P6105).

3. Results and discussions

3.1. The yields of hydroxyl radicals, hydrogen peroxide and ozone

3,4-Dihydroxybenzoic acid (DHDB) is the product of 4-hydroxybenzoate (HDB) trapping hydroxyl radicals. Higher DHDB concentration means more hydroxyl radical trapped [32]. Fig. 4 shows the yields of DHDB in the different discharged reactors. It is seen that the yield is lowest in reactor I without bubbling, which is in accordance with the result presented in the former work [32]. With bubbling gas flow of 120 L h^{-1}, the yield is much higher in reactor I than that in reactor II. The original formation rate of hydroxyl radical, which is obtained by linearly fitting the figures in Fig. 2, is 7.56×10^{-8} mol L^{-1} s^{-1} in reactor II, 2.27×10^{-7} mol L^{-1} s^{-1} in reactor I with bubbling gas and 5.06×10^{-8} mol L^{-1} s^{-1} in reactor I without bubbling, respectively.

Fig. 5 shows the variation of hydrogen peroxide concentration in the distilled water in the two different reactors. It is seen that hydrogen peroxide is highest in reactor I without bubbling at the same discharge time, which was caused by most of the discharge energy was obtained by water molecules and was consistent with the result present in former work [32]. But it was confirmed that the salt content had badly affection on the formation of active species and organic contaminant degradation in the non-bubbling reactor [36]. When increasing the salt concentration higher than 1.0×10^{-3} mol L^{-1}, the formation rates of hydroxyl radical and hydrogen peroxide and 4-CP degradation had little change in the bubbling reactor, but the rates decreased to nearly zero and the 4-CP was hardly removed in the non-bubbling reactor for most of the input energy was gained by ions [36]. In addition, it was known from the above that the formation rate of hydroxyl radical was lower in reactor without bubbling than that with bubbling. It was considered that the hydroxyl radical was more advantageous for 4-CP degradation [4].

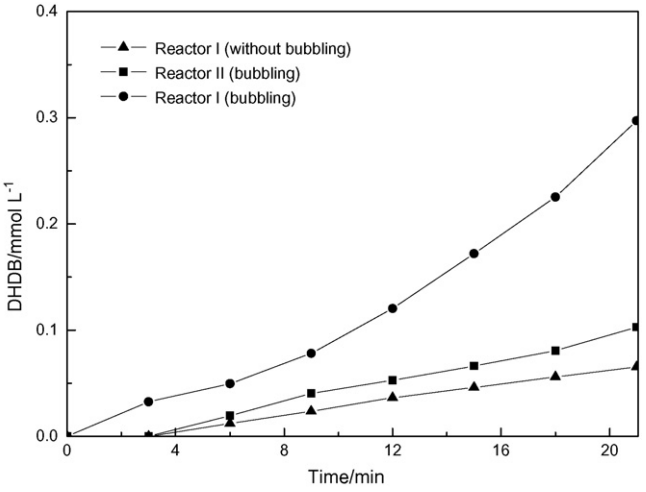

Fig. 4. The yields of DHDB in different reactors.

The hydrogen peroxide concentration is increased with time. The formation of hydrogen peroxide is determined by the processing parameters in the discharge system and is zero-order while keeping the parameters invariant [4,6]. Hydrogen peroxide is not increased in line in the two reactors with bubbling because it can be decomposed by the liquid chemical process. The concentration is higher before 12 min and is lower after 12 min in reactor I with bubbling than that in reactor II, resulting that the dissociation rate of hydrogen peroxide was higher in the former reactor. The original H_2O_2 formation rates were calculated by fitting the figures in the

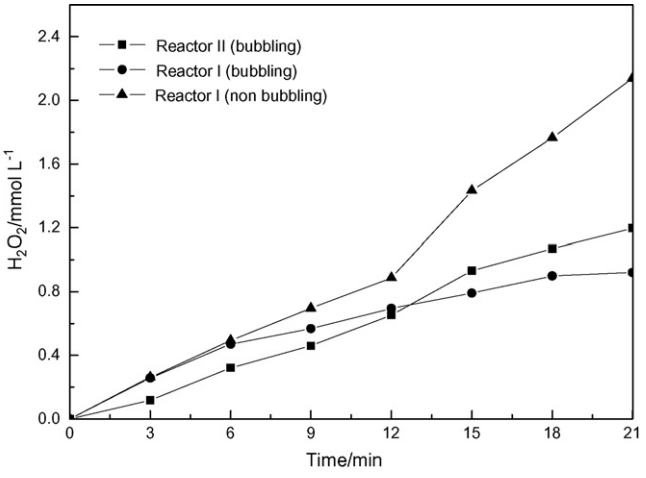

Fig. 5. The yields of hydrogen peroxide in different reactors.

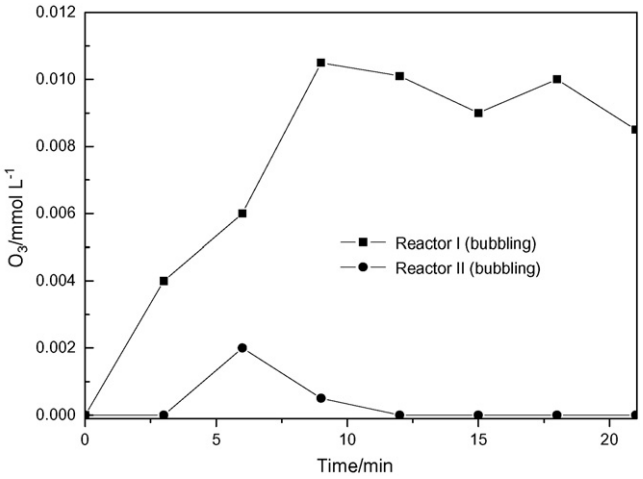

Fig. 6. The yields of ozone in different reactors.

first 6 min in the Fig. 5, which was 3.27×10^{-6} mol s^{-1} L^{-1} in reactor I with bubbling and was 2.23×10^{-6} mol s^{-1} L^{-1} in reactor II.

Fig. 6 shows the concentration of ozone during discharge in distilled water. It is seen that there is little ozone formed in reactor II. The best value of ozone yield was only 2.00×10^{-6} mol L^{-1}. But much more ozone is formed in reactor I. The ozone is increased fast in 12 min, and the best value of 1.05×10^{-5} mol L^{-1} was achieved at 9 min. Little variation was caused from 9 to 21 min. In experiments, the ozone concentration was more than 300 ppm in the escaped gas and was very close in reactors I and II. The original O_3 formation rate in reactor I was evaluated by fitting the figures in the first 9 min in Fig. 6, which was 1.87×10^{-8} mol s^{-1} L^{-1}. There was no ozone detected in the liquid when no gas was bubbled into the reactor showing the result that the ozone was formed by the bubbling gas getting energy from the discharge.

In order to compare the discharge energy efficiency in different reactor, the energy efficiency of hydroxyl radical (G_{OH}), hydrogen peroxide ($G_{H_2O_2}$) and ozone (G_{O_3}) are evaluated by the formation rate of the hydroxyl radical (r_{OH}), hydrogen peroxide ($r_{H_2O_2}$) or ozone (r_{O_3}), respectively, divided by energy input:

$$G_{OH} = \frac{r_{OH}}{SED}$$

$$G_{H_2O_2} = \frac{r_{H_2O_2}}{SED}$$

$$G_{O_3} = \frac{r_{O_3}}{SED}$$

where SED is the specific energy density, which is defined as:

$$SED = \frac{W_p}{Q}$$

where Q is the solution value in the discharge reactor (300 mL in this paper) and W_p is the input power from power supply to the reactor and is calculated using the following equation [37]:

$$W_P = \frac{1}{2} C U^2 f$$

where C is storage capacitance, U is the input voltage and f is the frequency.

The energy efficiency of hydrogen peroxide and ozone in different reactor are listed in Table 1. In some references, the ozone or the hydrogen peroxide was presented as concentration at certain discharge time, though the $r_{H_2O_2}$ or r_{O_3} is evaluated by the concentration divided the discharge time.

In the reactor used in present study, the discharge electrodes were five solid needles which were covered by capillaries through which gas was supplied to the discharge region, forming gas bubbles. The needle tips were only 0.5 mm higher than the five capillaries. When gas was bubbled into the reactor through the aeration capillaries, the discharge needles and their tips were surrounded by the bubbling gas and the gas was surrounded by water. As the discharge occurred, the gas molecules in the discharge region were dissociated or excited to form gas plasma [11,40–42]:

$$e + O_2 \rightarrow 2e + O_2^+ \quad (1)$$

$$e + O_2 \rightarrow 2e + O(^1D) + O^+ \quad (2)$$

The ozone is formed in bubbles by the following reaction:

$$O(^1D) + O_2 \rightarrow O_3 \quad (3)$$

The rate of the reaction is determined by the processing parameters in the discharge system and is zero-order while keeping the parameters invariant. Because the capillaries were only 1.0 mm in diameter, the gas flow was very slim and surrounded by water. The excited species formed in gas-phase were trapped immediately by the water molecules and the ozone transmitted into water phase [42]:

$$O(^1D) + H_2O \rightarrow H_2O_2 \quad (4)$$

$$O(^1D) + H_2O \rightarrow 2OH^\bullet \quad (5)$$

$$O_3 \rightarrow O_3(aq) \quad (6)$$

A little water molecules in the discharge region could also get energy directly [4,6].

$$H_2O \xrightarrow{e} {}^\bullet OH + H^\bullet \quad (7)$$

$$2H_2O \xrightarrow{e} H_2O_2 + 2H \quad (8)$$

The transfer of the ozone from bubbles into the liquid was limited by mass transfer coefficient and mass transfer interface between bubbles and water, which was determined by the characteristic and the processing parameter of the reactor. In one experiment, the characteristic and the processing parameter of the

Table 1
The G_{OH} ($\times 10^{-9}$ mol L^{-1} W^{-1}), $G_{H_2O_2}$ ($\times 10^{-8}$ mol L^{-1} W^{-1}) and G_{O_3} ($\times 10^{-9}$ mol L^{-1} W^{-1}) in different reactors

SED (W L^{-1})	r_{OH} ($\times 10^{-8}$)	$r_{H_2O_2}$ ($\times 10^{-7}$)	r_{O_3} ($\times 10^{-8}$)	G_{OH}	$G_{H_2O_2}$	G_{O_3}	Refs.
175	22.7	32.7	1.87	1.30	1.87	0.11	The paper (reactor I)
175	7.56	22.3	1.11	0.43	1.27	0.06	The paper (reactor II)
154	0.11	1.22	–	0.01	0.08	–	Joshi et al. [4]
220.9	–	4.90	–		0.22	–	Lukes et al. [25]
63.89	6.7	6.1	–	1.05	0.95	–	Sahni et al. [30]
155.8	–	13.80	0.18	–	0.89	0.01	Grymonpre et al. [27]
70.8	–	10.40	1.22	–	1.47	0.17	Zhang et al. [28]
1600	–	1.76	3.85	–	0.01	0.02	Wang et al. [38]
176.4	–	7.30	–	–	0.41	–	Wang et al. [39]

Note: The unit for r_{OH}, $r_{H_2O_2}$ and r_{O_3} is mol L^{-1} s^{-1}.

reactor can be seen as invariant except the temperature. Generally, the liquid temperature in the reactor will be increased with the discharge without any cooling method. The transfer of ozone from bubbling gas into the liquid could be decreased with the increase in temperature [39]. Additionally, the ozone could be decomposed in the discharged water [42]:

$$O_3 \xrightarrow{h\nu} O_2 + O(^1D) \quad (9)$$

$$O_3 + H_2O \xrightarrow{h\nu} O_2 + H_2O_2 \quad (10)$$

Therefore, the ozone concentration in the liquid is not still increased with discharge time. The ozone in the escaped gas of reactor I was similar to that in reactor II, which means that the energy obtained by oxygen gas was the same in the two reactors. But the concentration of dissolved ozone in the liquid was much higher in the former reactor. The ground electrode in reactor I was stainless steel wire mesh with same diameter as the inner diameter of the reactor, while it was a stainless steel plate with diameter 20 mm less than the inner diameter of the reactor. It was observed that the bubbling gas flew up to the ground electrode, gathering on the back surface of the plate electrode to form bigger bubbles, and flew around the plate through the gap between the edge of the plate and wall of the reactor in reactor II. But in reactor I, the bubbles flew through the pores of the mesh and were split into thinner bubbles. Therefore, the character of mass transfer was much better in reactor I than that in reactor II. More ozone could transfer into the liquid in reactor I, due to which the ozone concentration was much higher in reactor I than that in reactor II. In addition, better transfer characteristic between liquid and gas in reactor I could make more active species such as $O^{\bullet}$, $H^{\bullet}$ and high energy electrons to transfer into liquid to take part in the liquid chemical process. Therefore, the original formation rates of hydroxyl radical and hydrogen peroxide were all higher in reactor I than that in reactor II with bubbling.

Comparing Fig. 2 with Fig. 3, related results are found between the yields of the hydroxyl radical and hydrogen peroxide. They all increased in line with time in reactors I and II. In reactor I, hydrogen peroxide is increased in line in 6 min, but it is increased very slowly after 6 min. By contrast, the yield of hydroxyl radical yields is increased slowly in 6 min, but it is increased faster after discharge for 6 min. As soon as it is formed, the hydrogen peroxide could be dissociated [4]:

$$H_2O_2 \xrightarrow{e} H^{\bullet} + HO_2^{\bullet} \quad (11)$$

$$H_2O_2 \xrightarrow{e} OH^{\bullet} + OH^- \quad (12)$$

It is seen from Fig. 3 that more hydrogen peroxide is generated in reactor I, but the dissociation is more evident, which speeds up the formation of hydroxyl radical.

3.2. 4-CP degradation

Fig. 7 shows 4-CP degradation in the two reactors. It is seen that 4-CP concentration has little variation in reactor I in the absence of electrical discharge. Similar results were obtained in reactor II if the electrical discharge was not applied. As the electrical discharge was supplied in the two reactors, the concentration of 4-CP was decreased during 36 min. It is seen that the concentration of 4-CP is decreased much faster in reactor I than that in reactor II. It was clear from the above that there were much more active species generated in reactor I than that in reactor II with bubbling. More active species could make 4-CP degradation faster. About 97% 4-CP was removed at 36 min in reactor I, but only 70% 4-CP was removed at same time in reactor II. With 4-CP degradation, chloride ions were released. It is seen from Fig. 7 that the concentration of free chloride ions is increased with decrease in 4-CP concentration in reactor I.

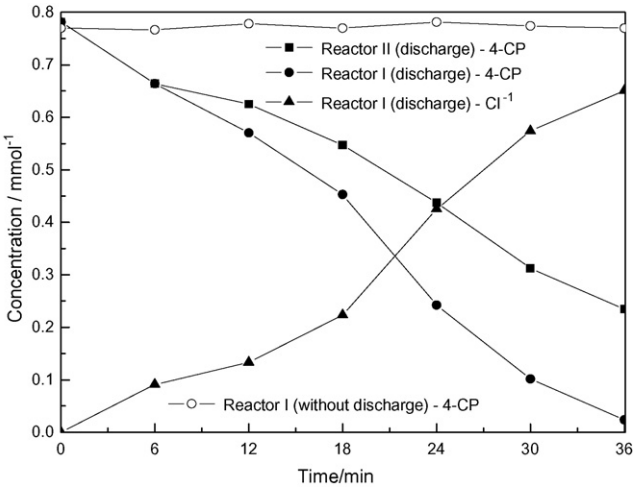

Fig. 7. The 4-CP degradation in different reactors.

3.3. The process of 4-CP degradation in reactor I with bubbling

3.3.1. The effect of bubbling gas on 4-CP degradation

Fig. 8 shows 4-CP degradation at different flows of bubbling gas. It is seen that bubbling gas has a great influence on 4-CP degradation. Only 46.0% 4-CP was removed at 30 min with no gas bubbled into the reactor, while more than 64% 4-CP was removed at the bubbling gas flow rate of 80 L h^{-1} and more than 85% 4-CP was removed at the rate of 120 and 160 L h^{-1} at the same discharge time. It was clear from the above that bubbling gas could make ozone and much more $^{\bullet}OH$ generated in the reactor during discharge, which could speed up the degradation of 4-CP. Therefore, the bubbling reactor was preferred in the present work. As the discharge occurred, the gas molecules around the tips of the discharge needles could get energy and be dissociated because the needle tips are very thin and the energy transmitted by the tips is limited. Higher bubbling flux does not mean more dissociation of oxygen molecules. In experiments, it was found that the solution could be dripping through the aeration capillaries into the gas chamber at the bubbling flux of 80 L h^{-1}. It is also seen from Fig. 8 that 4-CP degradation at 160 L h^{-1} is very close to that at 120 L h^{-1}. Higher bubbling flux means more wastage energy. Therefore, bubbling flux is kept at 120 L h^{-1} in the following experiments.

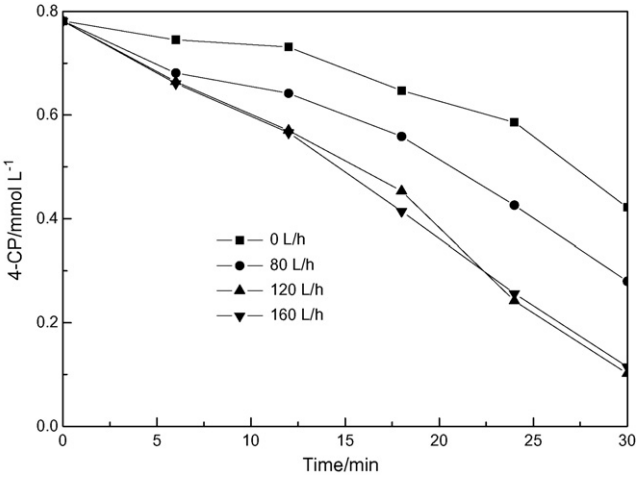

Fig. 8. The effect of bubbling gas on 4-CP degradation.

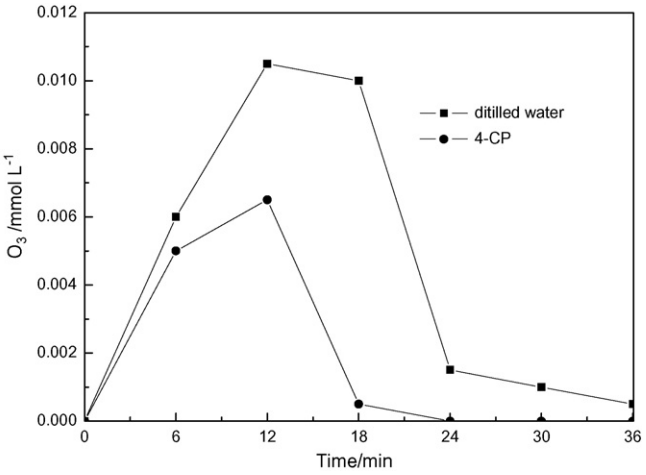

Fig. 9. The variation of ozone concentration in original solution of distilled water and 100 mg L^{-1} 4-CP.

3.3.2. Utilization of ozone and hydrogen peroxide in 4-CP degradation

Ozone is an oxidant. The second reaction rate between ozone and 4-CP is 6.0×10^2 L mol^{-1} s^{-1} [32]. Therefore, the ozone formed by discharge could react with 4-CP. Fig. 9 shows the variations of ozone concentration in distilled water and 4-CP solution. It is seen that the ozone concentration is higher in the former than that in the latter at same discharge time. The maximum value of ozone in distilled water was 1.05×10^{-5} mol L^{-1}, while it was 6.5×10^{-6} mol L^{-1} in 4-CP degradation process.

Similar results were obtained for hydrogen peroxide. Fig. 10 shows the concentrations of hydrogen peroxide in distilled water and 4-CP solution. It is seen that the concentration of hydrogen peroxide is much lower in 4-CP degradation process than that in distilled water, with the result that most of the ozone and hydrogen peroxide could be utilized by the degradation process of 4-CP during discharge.

3.3.3. The production of organic acid

Organic acids such as formic, acetic, oxalic, propanoic and maleic acid were generated in 4-CP degradation process, which could make variation in pH and conductivity. Variation in pH and conductivity during 4-CP degradation is shown in Fig. 11. It is seen that pH was

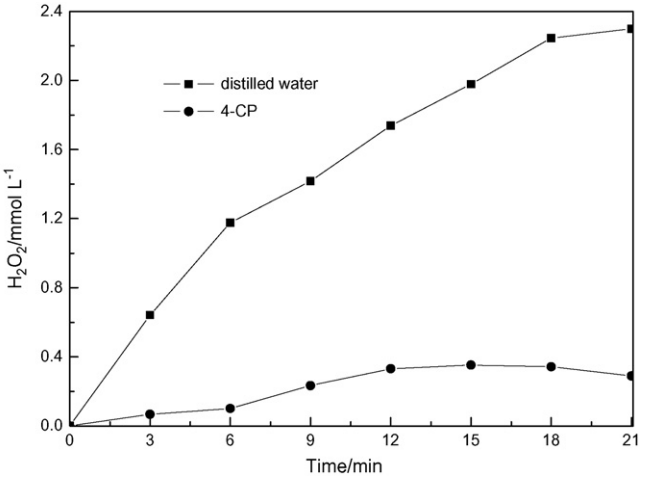

Fig. 10. The variation of hydrogen peroxide concentration in original solution of distilled water and 100 mg L^{-1} 4-CP.

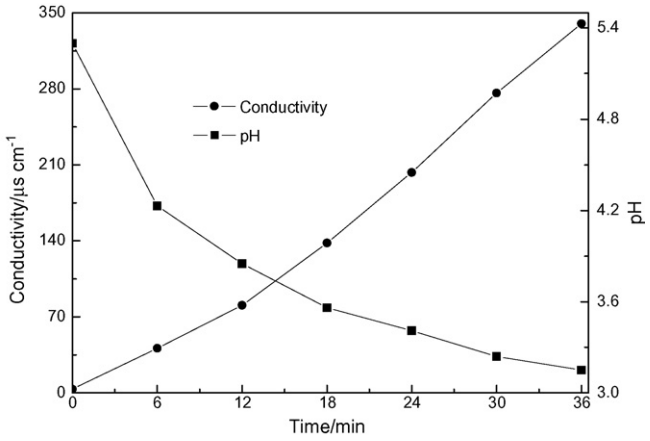

Fig. 11. The variation in pH and conductivity during 4-CP degradation.

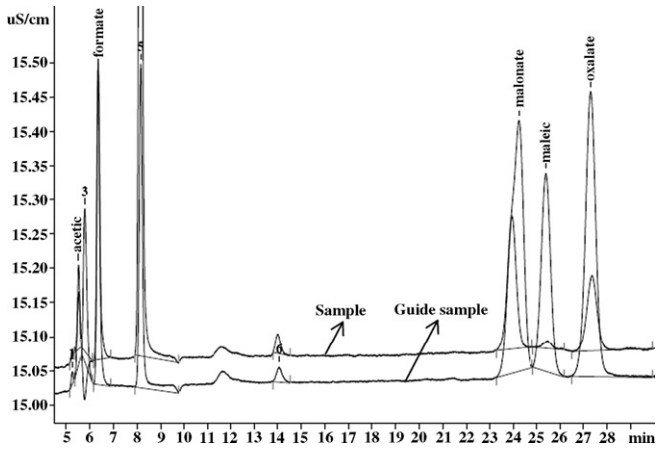

Fig. 12. IC chromatographic chromatogram of guide and 4-CP degradation sample.

decreased but the conductivity was increased with the discharge time.Fig. 12 shows the IC chromatographic chromatogram of guide sample and discharged sample. Fig. 13 shows the variation in the concentrations of formic, oxalic and propanoic acid during 36 min discharge. It is seen that there is no maleic acid generated in the first 6 min discharge. The concentration of maleic acid is increased slowly from 12 to 24 min, but it is increased quickly at 30 min. At 36 min, there was 0.032 mmol L^{-1} maleic acid formed. There is a clear turning point in the concentration of propanoic acid. Its con-

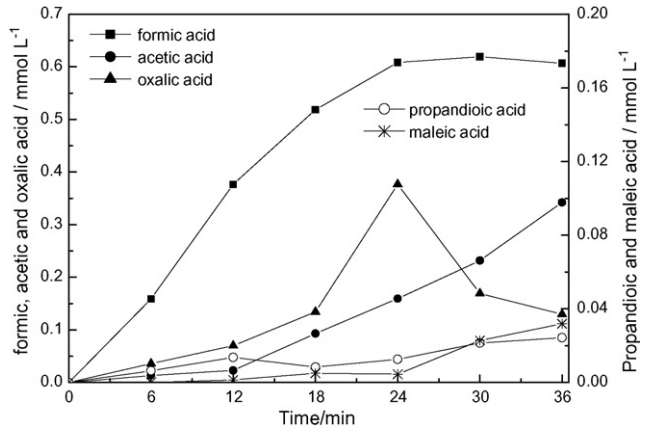

Fig. 13. The yields of formic, acetic, oxalic, propanoic and maleic acid during 4-CP degradation.

centration is increased before 24 min and then decrease steeply. Before 24 min, the concentration of propanoic acid is higher than that of oxalic acid. But after the turning point, the concentration of propanoic acid is lower than that of oxalic acid. At 36 min, the yield of propanoic acid was about 0.13 mmol L^{-1}. The oxalic acid is still increased in the 36 min discharge. In the first 12 min, it is very low in the liquid, but it is almost increased in line after 12 min. At 36 min, its yield was about 0.34 mmol L^{-1}. The yields of acetic were very low in the liquid. The highest concentration for acetic acid was only 0.024 mmol L^{-1}. The yields of formic acid were very high. It increases almost in line in the first 18 min, and the increasing trend was smoothed between 18 and 24 min. After 24 min, the concentration of formic acid was almost kept invariable in the liquid. At 36 min, the yield of formic acid was about 0.61 mmol L^{-1}.

4. Conclusion

The formation yields of active specie such as ozone, hydrogen peroxide and hydroxyl radical was higher in reactor I with bubbling gas, which sped up the 4-CP degradation. About 97% 4-CP was removed at 36 min in reactor I, while only 70% 4-CP was removed at same time in reactor II. Some organic acids such as formic, acetic, oxalic, propanoic and maleic acid were generated during 4-CP degradation, which cause a decrease in the pH and an increase in the conductivity. At 36 min, the yields of formic, acetic, oxalic, propanoic and maleic acid were about 0.61, 0.34, 0.024, 0.13 and 0.032 mmol L^{-1}, respectively.

Acknowledgment

This work was partially supported by Key Academic Discipline of Organic Chemistry of Jiangsu Province.

References

[1] J.S. Clenments, Preliminary investigation of prebreakdown phenomena and chemical reactions using a pulsed high-voltage discharge in water, IEEE Trans. Ind. Appl. 23 (1987) 224–235.
[2] B. Sun, M. Sato, A. Harano, J.S. Clements, Non-uniform pulse discharge-induced radical production in distilled water, J. Electrostat. 21 (2001) 345–354.
[3] B. Sun, M. Sato, Use of a pulsed high-voltage discharge for removal of organic compounds in aqueous solution, J. Phys. D: Appl. Phys. 32 (1999) 1908–1915.
[4] A.A. Joshi, B.R. Locke, P. Arce, W.C. Finney, Formation of hydroxyl radicals, hydrogen peroxide and aqueous electrons by pulsed streamer corona discharge in aqueous solution, J. Hazard. Mater. 41 (1995) 3–30.
[5] M. Sato, T. Ohgiyama, J.S. Clements, Formation of chemical species and their effects on microorganisms using a pulsed high-voltage discharge in water, IEEE Trans. Ind. Appl. 32 (1996) 106–112.
[6] B. Sun, M. Sato, J.S. Clements, Optical study of active species produced by a pulsed streamer corona discharge in water, J. Electrostat. 39 (1997) 189–202.
[7] L.V. Lisitsyn, H. Nomiyama, S. Katsuki, H. Akiyama, Thermal process in a streamer discharge in water, IEEE Trans. Dielectr. Electr. Insulat. 6 (1999) 351–356.
[8] X. Lu, K. Liu, M. Liu, Y. Pan, H. Zhang, Research on high density plasma of pulsed discharge in water, Pulsed Power Plasma Sci. 2 (2001) 1595–1598.
[9] A.T. Sugiarto, M. Sato, Pulsed plasma processing of organic compounds in aqueous solution, Thin Solid Films 386 (2001) 295–299.
[10] D. Hemmert, K. Shiraki, T. Yokoyama, S. Katsuki, H. Bluhm, H. Akiyama, Optical diagnostics of shock waves generated by a pulsed streamer discharge in water, in: Pulsed Power Conference, 14th IEEE International, vol. 1, 2003, pp. 232–235.
[11] Y.S. Mok, C.M. Nam, M.H. Cho, I.S. Nam, Decomposition of volatile organic compounds and nitric oxide by nonthermal plasma discharge process, IEEE Trans. Plasma Sci. 30 (2002) 408–415.
[12] P. Sunka, V. Babicky, M. Clupek, M. Fuciman, J. Schmidt, J. Benes, Generation of focused shock waves by multi-channel discharges in water, Pulsed Power Plasma Sci. 2 (2001) 1134–1137.
[13] N. Sano, T. Kawashima, J. Fujikawa, T. Fujimoto, T. Kitai, T. Kanki, Decomposition organic compounds in water by direct contact of gas corona discharge: influence of discharge condition, Ind. Eng. Chem. Res. 41 (2002) 5906–5911.
[14] A.T. Sugiarto, T. Ohshima, M. Sato, Advanced oxidation processes using pulsed streamer corona discharge in water, Thin Solid Films 407 (2002) 174–178.
[15] D.C. Yee, S. Chauhan, E. Yankelevich, V. Bystritskii, K.T. Wood, Degradation of perchloroethylene and dichlorophenol by pulsed-Electric discharge and bioremediation, Biotechnol. Bioeng. 59 (1998) 438–444.
[16] D.M. Willberg, P.S. Lang, Degradation of 4-chlorophenol, 3,4-dichloroaniline, and 2,4,6-trinitrotoluene in an electrohydraulic discharge reactor, Environ. Sci. Technol. 30 (1996) 2526–2534.
[17] P.S. Lang, D.M. Willberg, Oxidative degradation of 2,4,6-trinitrotoluene by ozone in an electrohydraulic discharge reactor, Environ. Sci. Technol. 32 (1998) 3142–3148.
[18] N. Sano, D. Yamamoto, T. Kanki, Decomposition of phenol in water by a cylindrical wetted-wall reactor using direct contact of gas corona discharge, Ind. Eng. Chem. Res. 42 (2003) 5423–5428.
[19] E. Njatawidjaja, A.T. Sugiarto, T. Ohshima, M. Sato, Decoloration of electrostatically atomized organic dye by the pulsed streamer corona discharge, J. Electrostat. 63 (2005) 353–359.
[20] J. Li, M. Sato, T. Ohshima, Degradation of phenol in water using a gas–liquid phase pulsed discharge plasma reactor, Thin Solid Films 515 (2007) 4283–4288.
[21] A.K. Sharma, B.R. locke, P. Arce, W.C. Finney, A preliminary study of pulsed streamer corona discharge for degradation of phenol in aqueous solution, Hazard Waste Harzard. Mater. 10 (1993) 209–219.
[22] A. Mizuno, Y. Hori, Destruction of living cells by pulsed high-voltage application, IEEE Trans. Ind. Appl. 24 (1988) 387–394.
[23] Y.Z. Wen, X.Z. Jiang, Degradation of 4-chorophenol by high-voltage pulse corona discharges combined with ozone, Plasma Chem. Plasma Process. 22 (2002) 175–185.
[24] D.R. Grymonpre, W.C. Finney, B.R. Locke, Aqueous-phase pulsed streamer corona reactor using suspended activated carbon particles for phenol oxidation: model-data comparison, Chem. Eng. Sci. 54 (1999) 3095–3105.
[25] P. Lukes, A. Appleton, B.R. Locke, Hydrogen peroxide and ozone formation in hybrid gas–liquid electrical discharge reactors, IEEE Trans. Ind. Appl. 40 (2004) 60–67.
[26] P. Lukes, B.R. Locke, Degradation of substituted phenols in hybrid gas–liquid electrical discharge reactor, Ind. Eng. Chem. Res. 44 (2005) 2921–2930.
[27] D.R. Grymonpré, W.C. Finney, R.J. Clark, B.R. Locke, Hybrid gas–liquid electrical discharge reactors for organic compound degradation, Ind. Eng. Chem. Res. 43 (2004) 1975–1989.
[28] Y. Zhang, J. Zheng, X. Qu, H. Chen, Design of a novel non-equilibrium plasma-based water treatment reactor, Chemosphere 70 (2008) 1518–1524.
[29] M. Sahni, B.R. Locke, The effects of reaction conditions on liquid-phase hydroxyl radical production in gas–liquid pulsed-electrical-discharge reactors, Plasma Process. Polym. 3 (2006) 668–681.
[30] M. Sahni, B.R. Locke, Quantification of hydroxyl radicals produced in aqueous phase pulsed electrical discharge reactors, Ind. Eng. Chem. Res. 45 (17) (2006) 5819–5825.
[31] S.M. Line, B. Daniel, V. Luc, M. Jane, Evaluation of sodium 4-hydroxylbenzoate as an hydroxyl radical trap using gas chromatography-mass spectrometry and high-performance liquid chromatography with electrochemical detection, Anal. Biochem. 241 (1996) 67–74.
[32] W. Bian, M. Zhou, L. Lei, Formations of active species and by products in water by pulsed high-voltage discharge, Plasma Chem. Plasma Process. 27 (2007) 337–348.
[33] M.S. Robin, Spectrophotometric determination of hydrogen peroxide using potassium titanium (IV) oxalate, Analyst 105 (1980) 950–954.
[34] H. Bader, J. Hoigne, Determination of ozone in water by the indigo method, Water Res. 15 (1981) 449–456.
[35] State environmental protection administration of China, in: Analytical Method for Air and Exhausted Gas Monitor (Chinese), China Environmental Science Press, Beijing, 2003, pp. 133–137.
[36] W. Bian, L. Lei, An electrohydraulic discharge system of salt-resistance for *p*-chlorophenol degradation, J. Hazard. Mater. 148 (2007) 178–184.
[37] M.A. Malik, U. Rehman, A. Ghaffar, K. Ahmed, Synergistic effect of pulsed corona discharges and ozonization on decolourization of methylene blue in water, Plasma Sources Sci. 11 (2002) 236–240.
[38] C. Wang, Y. Wu, G. Li, Inactivation of *E. coli* with plasma generated by bipolar pulsed discharge in a three-phase discharge plasma reactor, J. Electrostat. 66 (2008) 71–78.
[39] H. Wang, J. Li, X. Quan, Y. Wu, G. Li, F. Wang, Formation of hydrogen peroxide and degradation of phenol in synergistic system of pulsed corona discharge combined with TiO_2 photocatalysis, J. Hazard. Mater. 141 (2007) 336–343.
[40] R. Burlica, M.J. Kirkpatrick, B.R. Locke, Formation of reactive species in gliding arc discharges with liquid water, J. Electrostat. 64 (2006) 35–43.
[41] Z. He, J. Liu, W. Cai, The important role of the hydroxy ion in phenol removal using pulsed corona discharge, J. Electrostat. 63 (2005) 371–386.
[42] X.H. Xu, W.R. Zhao, Water and Wastewater Treatment with Ozone, Chemical Industry Press of China, Beijing, 2003, p. 337.